

Hsa_circ_0054633 regulates PDGF-BB-induced proliferation, migration and oxidative stress of vascular smooth muscle cells through miR-107/TXNIP axis

Type

Research paper

Keywords

Oxidative stress, miR-107, hsa_circ_0054633, TXNIP, HA-VSMCs

Abstract

Introduction

Hsa_circ_0054633 has been found to be elevated in the blood of coronary artery disease (CAD) patients. However, the molecular mechanism and the role of hsa_circ_0054633 in the pathogenesis of CAD have not been reported in detail.

Material and methods

The expression of hsa_circ_0054633, microRNA (miR)-107 and thioredoxin-interacting protein (TXNIP) mRNA was measured using quantitative real-time polymerase chain reaction. Human artery vascular smooth muscle cell (HA-VSMC) proliferation, cell cycle, and migration were detected by cell counting kit-8 assay, flow cytometry and transwell assay, respectively. The generation of reactive oxygen species (ROS) was analyzed by dichlorofluorescein diacetate (DCFH-DA) assay. Western blot was utilized to determine the levels of proliferating cell nuclear antigen (PCNA), cyclin D1, matrix metalloproteinase 9 (MMP-9), Mn-superoxide dismutase (SOD2) and TXNIP protein. The interaction between miR-107 and hsa_circ_0054633 or TXNIP was confirmed by dual-luciferase reporter, RNA immunoprecipitation assay or pull-down assay.

Results

Hsa_circ_0054633 was elevated in the plasma of CAD patients, and might be a potential blood biomarker for CAD prediction. Hsa_circ_0054633 silencing reversed PDGF-BB-induced promotion on HA-VSMC proliferation, cell cycle, migration and ROS production. MiR-107 directly interacted with hsa_circ_0054633 and TXNIP, and hsa_circ_0054633 regulated TXNIP expression by sponging miR-107. Besides, rescue assay indicated that the action of hsa_circ_0054633 silencing on PDGF-BB-treated HA-VSMCs could be attenuated by miR-107 inhibition or TXNIP overexpression, respectively.

Conclusions

Hsa_circ_0054633 knockdown protected HA-VSMCs against PDGF-BB-induced dysfunction through regulating miR-107/TXNIP axis, suggesting a potential therapeutic target for coronary atherosclerosis.

1 **Hsa_circ_0054633 regulates PDGF-BB-induced proliferation, migration and**
2 **oxidative stress of vascular smooth muscle cells through miR-107/TXNIP axis**

3 Xiaochun Lei¹, Yi Ding², Ye Tian³, Peng Ding^{1*}

4 ¹Department of Cardiovascular Medicine, The Second Affiliated Hospital of Xi'an
5 Medical University, Xi'an, Shaan'xi, China.

6 ²Department of Nephrology and Endocrinology, The Second Affiliated Hospital of
7 Xi'an Medical University, Xi'an, Shaan'xi, China.

8 ³Department of Neurology, The Second Affiliated Hospital of Xi'an Medical University,
9 Xi'an, Shaan'xi, China.

10 ***Corresponding author:** Peng Ding. Department of Cardiovascular Medicine, The
11 Second Affiliated Hospital of Xi'an Medical University, No. 167 Fangdong Street,
12 Baqiao District 710038, Xi'an, Shaan'xi, China.

13 **Tel:** +86-15029002153 **Email:** zlqwr5@163.com

14 **Running title:** Hsa_circ_0054633 regulates PDGF-BB-induced dysfunction of HA-
15 VSMCs.

16

17 **Abstract**

18 **Introduction:** Hsa_circ_0054633 has been found to be elevated in the blood of
19 coronary artery disease (CAD) patients. However, the molecular mechanism and the
20 role of hsa_circ_0054633 in the pathogenesis of CAD have not been reported in detail.

21 **Materials and Methods:** The expression of hsa_circ_0054633, microRNA (miR)-107
22 and thioredoxin-interacting protein (TXNIP) mRNA was measured using quantitative

23 real-time polymerase chain reaction. Human artery vascular smooth muscle cell (HA-
24 VSMC) proliferation, cell cycle, and migration were detected by cell counting kit-8
25 assay, flow cytometry and transwell assay, respectively. The generation of reactive
26 oxygen species (ROS) was analyzed by dichlorofluorescein diacetate (DCFH-DA)
27 assay. Western blot was utilized to determine the levels of proliferating cell nuclear
28 antigen (PCNA), cyclin D1, matrix metalloproteinase 9 (MMP-9), Mn-superoxide
29 dismutase (SOD2) and TXNIP protein. The interaction between miR-107 and
30 hsa_circ_0054633 or TXNIP was confirmed by dual-luciferase reporter, RNA
31 immunoprecipitation assay or pull-down assay.

32 **Results:** Hsa_circ_0054633 was elevated in the plasma of CAD patients, and might be
33 a potential blood biomarker for CAD prediction. Hsa_circ_0054633 silencing reversed
34 PDGF-BB-induced promotion on HA-VSMC proliferation, cell cycle, migration and
35 ROS production. MiR-107 directly interacted with hsa_circ_0054633 and TXNIP, and
36 hsa_circ_0054633 regulated TXNIP expression by sponging miR-107. Besides, rescue
37 assay indicated that the action of hsa_circ_0054633 silencing on PDGF-BB-treated
38 HA-VSMCs could be attenuated by miR-107 inhibition or TXNIP overexpression,
39 respectively.

40 **Conclusion:** Hsa_circ_0054633 knockdown protected HA-VSMCs against PDGF-BB-
41 induced dysfunction through regulating miR-107/TXNIP axis, suggesting a potential
42 therapeutic target for coronary atherosclerosis.

43 **Keywords:** hsa_circ_0054633, miR-107, TXNIP, oxidative stress, HA-VSMCs

44

45 **Introduction**

46 Coronary artery disease (CAD) is a leading cause of mortality in the world. Despite
47 great improvements in prevention, medical and interventional management, the
48 incidence and mortality of CAD remain increasing in recent years [1, 2].
49 Atherosclerosis (AS) is a chronic inflammatory disease of the arterial wall,
50 characterized by plaque formation, and is the well-recognized primary cause of CAD
51 [3]. The pathogenesis of AS lesion formation is complex, and the initiating phase of AS
52 plaques formation is the result of vascular smooth muscle cells (VSMCs) dysfunction
53 [4]. Increasing researches have revealed VSMCs damage is associated with the
54 regulation of atherosclerosis at tissue and molecular levels [5, 6]. Thus, better
55 understanding the molecular mechanism underlying abnormal VSMCs function is of
56 great significance for the development of new therapeutics.

57 Circular RNAs (circRNAs) are a type of endogenous non-coding RNAs derived
58 from reverse splicing of exons, introns or both [7, 8]. They have covalently closed loop
59 structures, which confer increasing stability relative to their linear transcripts [9].
60 Besides, many circRNAs are highly conserved and have tissue-specific expression
61 patterns. Importantly, growing evidence has documented that circRNAs play significant
62 roles in a variety of physiological and pathological processes, including cell cycle,
63 proliferation, migration, invasion, tumorigenesis, immune responses and oxidative
64 stress [10, 11]. Thus, circRNAs are ideal candidates for future diagnostic biomarkers
65 and therapeutic interventions [12]. Hsa_circ_0054633 is a novel identified circRNA.
66 Zhao *et al.* demonstrated that hsa_circ_0054633 was up-regulated in the peripheral

67 blood of type 2 diabetes mellitus (T2DM) patients, and was a potential blood biomarker
68 for pre-diabetes and T2DM prediction [13]. Pan *et al.* revealed that hsa_circ_0054633
69 down-regulation enhanced high glucose-mediated inhibition on proliferation, migration
70 and angiopoiesis of endothelial cells [14]. Importantly, Li *et al.* exhibited that
71 hsa_circ_0054633 expression was up-regulated in the blood of CAD patients [15].
72 However, the role of hsa_circ_0054633 on VSMCs dysfunction remains unclear.

73 Emerging studies have reported that platelet-derived growth factor-BB (PDGF-BB)
74 is one of the most potent stimulants for the dysfunction of VSMCs [16, 17]. Thus,
75 PDGF-BB was employed to induce VSMC dedifferentiation to mimic VSMC
76 dysfunction in coronary atherosclerosis *in vitro*. This study aimed to explore the
77 molecular mechanism and the role of hsa_circ_0054633 in PDGF-BB-induced VSMCs
78 dysfunction, thus investigating the potential roles of hsa_circ_0054633 in the presence
79 and progression of CAD.

80

81 **Materials and methods**

82 **Clinical samples**

83 A total of 33 patients with CAD were recruited from The Second Affiliated Hospital
84 of Xi'an Medical University. There were 19 males and 14 females, ranging in age from
85 30 to 75 years. All CAD patients were diagnosed by coronary angiography in line with
86 the guidelines established by American College of Cardiology/American Heart
87 Association. The exclusion criteria were as follows: (1) cancer and other severe diseases;
88 (2) serious infection within six weeks of the start of this work; (3) clinically acute or

89 active chronic inflammatory disease. In the same period, a total of 33 healthy
90 individuals were recruited to serve as the control group, and there were 18 females and
91 15 males with age ranging from 27 to 70 years.

92 Whole blood (20 ml) was extracted from each participant on the day of admission
93 to the study and transferred to anticoagulant tubes. Blood samples were centrifuged at
94 3000 g for 15 min, and plasma was collected in a plastic tube, followed by centrifuging
95 a second time at 3000 g for 15 min at room temperature. Subsequently, the plasma was
96 collected and stored at -80 °C before used. This study was approved by the Ethics
97 Committee of The Second Affiliated Hospital of Xi'an Medical University and written
98 informed consent was collected from all subjects.

99 **Cell culture and treatment**

100 Human artery vascular smooth muscle cells (HA-VSMCs) obtained from Chinese
101 Academy of Sciences (Shanghai, China) were maintained in Dulbecco's modified
102 Eagle's medium (DMEM, Invitrogen, Waltham, MA, USA), which was supplemented
103 with 10% fetal bovine serum (FBS) (Gibco, Carlsbad, CA, USA), at 37°C with 5%
104 CO₂. For the PDGF-BB group, HA-VSMCs were treated with 30 ng/mL PDGF-BB
105 (Sigma, St. Louis, MO, USA) for 6 h at 37°C.

106 **Quantitative real-time polymerase chain reaction (qRT-PCR)**

107 The extraction of total RNA from plasma and cultured HA-VSMCs was performed
108 using TRIzol reagent (Invitrogen). First-strand complementary DNA (cDNA) was
109 synthesized by using the Reverse Transcription System Kit (Takara, Dalian, China),
110 then cDNA amplification was conducted using SYBR Green I (Takara) on the ABI7500

111 system. The relative fold change in expression was assessed by $2^{-\Delta\Delta C_t}$ method and
112 normalized by glyceraldehyde-3-phosphate dehydrogenase (GAPDH) or U6 small
113 nuclear B noncoding RNA (U6). The primers obtained from Qiagen (Valencia, CA,
114 USA) were listed as followed: hsa_circ_0054633, F 5'-
115 TTGCTTTCTACACTTTCAGGTGAC-3' and R 5'-
116 GCTTTTTGTCTGTAGTCAACCACCA-3'; miR-107, F 5'-
117 GTTAAGTCAGAGCGGGGCTT-3', and R 5'-CACTCCGCTTTTTTCAGTGCC-3';
118 TXNIP, F 5'-GCCACACTTACCTTGCCAAT-3', and R 5'-TTGGATCCAGGAACG
119 CTAAC-3'; GAPDH, F 5'-GTCAACGGATTTGGTCTGTATT-3', and R 5'-
120 AGTCTTCTGGGTGGCAGTGAT-3'; U6, F 5'-CTCGCTTCGGCAGCACA-3', and
121 R 5'-AACGCTTCACGAATTTGCGT-3'.

122 Cell transfection

123 The mimic or inhibitor targeting miR-107 (miR-107 or anti-miR-107), and their
124 corresponding negative control (miR-NC and anti-NC) were purchased from RIBOBIO
125 (Guangzhou, China). Two forms of small interfering RNA (siRNA) were designed by
126 Invitrogen to target hsa_circ_0054633 covalent closed junction (si-circ#1, si-circ#2),
127 the same vector harboring a scrambled sequence was used as a negative control (si-NC).
128 Also, pcDNA-TXNIP overexpression vector (TXNIP) and pcDNA negative control
129 (vector) were synthesized by Invitrogen. Subsequently, the transfection was performed
130 by Lipofectamine 2000 (Invitrogen).

131 Cell counting kit-8 (CCK-8) assay

132 After transfection and/or treatment, cells (5000/well) were cultivated into a 96-well

133 plate overnight, and then interacted with 10 μ L CCK-8 solution (Dojindo Molecular
134 Technologies, Japan) at 37°C for another 2 h. Finally, the optical density of each well
135 at 450 nm was analyzed by a microplate reader.

136 **Flow cytometry**

137 Following transfection and/or treatment, cells (1×10^6) were trypsinized and
138 resuspended to obtain single-cell suspensions, then detached cells were fixed overnight
139 in 70% ethanol, followed by staining with propidium iodide (Cell Cycle Detection kit;
140 BD Biosciences, San Jose, CA, USA). Finally, quantitation of cell cycle distribution
141 was analyzed with a FACScan flow cytometer (BD Biosciences). The percentage of the
142 cells in G0/G1, S, and G2/M phases was counted with FlowJo software.

143 **Transwell assay**

144 After transfection and/or treatment, cells in 200 mL serum-free DMEM were
145 seeded into the upper chamber of a transwell insert (Cell Biolabs, Inc. Santiago, CA,
146 USA), then lower chamber was filled with 600 mL medium supplementing with 10%
147 FBS. Following incubation at 37°C with 5% CO₂ for 24 h, cells on the lower face of
148 the membranes were fixed and stained. Finally, migrated cells from 10 randomly
149 selected fields were counted by a microscope.

150 **Detection of reactive oxygen species (ROS)**

151 The production of ROS was measured by Dichlorofluorescein diacetate (DCFH-
152 DA) assay. Transfected and/or treated HA-VSMCs were suspended using 20 mM 2',7'-
153 Dichlorodihydrofluorescein diacetate (DCFH-DA; Sigma) for 30 min at 37°C in the
154 dark. After washing with PBS three times, the fluorescence intensity of the samples was

155 detected using a fluorescence microplate reader at 488 nm excitation wavelength and
156 525 nm emission wavelength, respectively.

157 **Western blot**

158 Total protein was extracted using RIPA buffer (Beyotime, Shanghai, China) from
159 cells, and protein concentrations were determined using the bicinchoninic acid (BCA)
160 Protein Assay kit (Takara). Protein extractions were separated by 12% sodium lauryl
161 sulfate-polyacrylamide gels (SDS-PAGE) and transferred to polyvinylidene difluoride
162 membranes (PVDF; Millipore, Billerica, MA, USA). Then membranes were interacted
163 with primary antibodies against proliferating cell nuclear antigen (PCNA) (1:5000,
164 ab29), cyclin D1 (1:10000, ab134175), matrix metalloproteinase 9 (MMP-9) (1:2000,
165 ab38898), Mn-superoxide dismutase (SOD2) (1:5000, ab13533), TXNIP (1:2000,
166 ab188865) (Abcam, Cambridge, MA, USA), and the secondary antibody anti-rabbit
167 IgG-horseradish peroxidase at a 1:1000 dilution (Sangon, Shanghai, China). β -actin
168 (1:2000, 4967, Cell Signaling Technology, Boston, MA, USA) was used as an internal
169 control.

170 **Dual-luciferase reporter assay**

171 The sequences of TXNIP 3'-UTR or hsa_circ_0054633 containing the wild-type
172 (wt) or mutant (mut) potential binding sites of miR-107 were amplified and subcloned
173 into pRL-TK luciferase reporter vector (Promega, Madison, WI, USA), respectively.
174 Then cells were placed in 24-well plates and co-transfected with 10 ng wt or mut
175 constructed luciferase vectors, and 40 nM of miR-107 mimic or miR-NC mimic. The
176 luciferase activity was measured by a dual luciferase assay kit (Promega) and

177 normalized by renilla luciferase activity.

178 **RNA immunoprecipitation (RIP) assay**

179 HA-VSMCs were lysed with RIP lysis buffer (Millipore, Billerica, MA, USA). Cell
180 lysis was co-immunoprecipitated with magnetic beads containing human anti-Ago2
181 antibody (Abcam). Normal mouse IgG (Millipore) was used as a negative control.
182 Finally, immunoprecipitated RNA was purified and subjected to qRT-PCR analysis.

183 **Pull-down assay**

184 Biotin (Bio)-miR-107 and Bio-NC were synthesized by GenePharma Company
185 (Shanghai, China), and then transfected into HA-VSMCs for 48 h. Subsequently, cells
186 were lysed, and the extracts were incubated with streptavidin-coated magnetic beads
187 (Invitrogen). After elution, the bead-bound RNA complex was isolated and subjected
188 for reverse transcription using qRT-PCR analysis.

189 **Statistical analysis**

190 All experiments were performed three times. Data were expressed as mean \pm
191 standard deviation (SD). Statistical differences in different groups were analyzed by
192 Student's *t* test or one-way analysis of variance (ANOVA) with GraphPad Prism 7
193 software. Receiver operating characteristic (ROC) curves were plotted to analyze the
194 diagnostic value of hsa_circ_0054633. $P < 0.05$ indicated statistically significant.

195

196 **Results**

197 **Demographic characteristics of CAD patients and controls**

198 In this study, the demographic data, laboratory parameters of CAD patients and

199 controls were summarized in Table 1. As expected, there were significant differences
200 in hypertension, total cholesterol, triglyceride, LDL-cholesterol (LDL-C), and high-
201 sensitivity C-reactive protein (Hs-CRP) between these two subgroups ($P < 0.01$).
202 However, other factors, including sex, age, body mass index, cigarette smoking,
203 drinking, diabetes mellitus, and HDL-C, were not significantly different ($P > 0.05$).

204 **Hsa_circ_0054633 expression is elevated in CAD patients and PDGF-BB-induced** 205 **HA-VSMCs**

206 The expression of hsa_circ_0054633 was detected and results showed
207 hsa_circ_0054633 expression was up-regulated in the plasma of CAD patients relative
208 to the plasma of healthy people (Fig. 1A). Moreover, ROC curves revealed that the area
209 under the ROC curve (AUC) was 0.762 (95% confidence interval (CI): 0.637-0.887),
210 the cut-off value was 1.615, and the sensitivity and specificity were 63.64% and 96.97%,
211 respectively (Fig. 1B). Furthermore, highly expressed hsa_circ_0054633 were
212 associated with smoking history, with symptoms of hypertension and diabetes mellitus,
213 and with total cholesterol ≥ 5.1 mmol/L and triglyceride ≥ 1.8 mmol/L ($P < 0.05$;
214 Table 2). Besides that, hsa_circ_0054633 expression was also up-regulated in PDGF-
215 BB-induced HA-VSMCs compared with the cells untreated with PDGF-BB (Fig. 1C).

216 **Hsa_circ_0054633 knockdown reverses PDGF-BB-induced HA-VSMCs** 217 **dysfunction**

218 To investigate the role of hsa_circ_0054633 in CAD, we knocked down
219 hsa_circ_0054633 in HA-VSMCs by transfecting with two forms of constructed si-
220 hsa_circ_0054633 plasmid (si-circ#1, si-circ#2). Then the effects of si-circ#1 and si-

221 circ#2 were determined, and qRT-PCR analysis showed both si-circ#1 and si-circ#2
222 remarkably declined hsa_circ_0054633 expression compared with the si-NC group (Fig.
223 2A). Subsequently, HA-VSMCs were treated with PDGF-BB, PDGF-BB + si-NC, or
224 PDGF-BB + si-circ#1 to assay cell cycle, proliferation, migration and ROS production,
225 and we found hsa_circ_0054633 silence overturned PDGF-BB-mediated enhancement
226 of hsa_circ_0054633 expression (Fig. 2B). After that, CCK-8 assay indicated
227 hsa_circ_0054633 knockdown attenuated PDGF-BB-induced promotion on HA-
228 VSMC proliferation (Fig. 2C). Flow cytometric analysis showed PDGF-BB reduced
229 the number of HA-VSMCs in the G0/G1 phase and increased the number of HA-
230 VSMCs in the S phase, suggesting PDGF-BB promoted cell cycle progression, while
231 this promotion was abated by hsa_circ_0054633 knockdown (Fig. 2D). Transwell assay
232 exhibited that the increase of migrated HA-VSMCs induced by PDGF-BB was
233 mitigated by the silencing of hsa_circ_0054633 (Fig. 2E). Besides that, we found
234 PDGF-BB induced the generation of ROS, while hsa_circ_0054633 knockdown
235 inhibited the production of ROS in HA-VSMCs (Fig. 2F). In addition, western blot
236 showed hsa_circ_0054633 down-regulation also decreased PDGF-BB-mediated up-
237 regulation of PCNA, cyclin D1, MMP9, and SOD2 (Fig. 2G), further indicating
238 hsa_circ_0054633 knockdown reversed PDGF-BB-induced proliferation, cell cycle,
239 migration and oxidative damage in HA-VSMCs.

240 **Hsa_circ_0054633 is a sponge of miR-107**

241 The molecular mechanisms underlying the action of hsa_circ_0054633 on HA-
242 VSMC properties were explored. According to the prediction of starBase online

243 program, we found miR-107 had the potential binding sites of hsa_circ_0054633 (Fig.
244 3A). The expression of miR-107 was detected and results showed miR-107 expression
245 was down-regulated in the plasma of CAD patients compared with the plasma from
246 healthy people (Fig. 3B), moreover, lowly expressed miR-107 was related to smoking
247 history, symptoms of hypertension, total cholesterol ≥ 5.1 mmol/L and triglyceride
248 ≥ 1.8 mmol/L ($P < 0.05$; Table 2). Also, PDGF-BB decreased the expression of
249 miR-107 in HA-VSMCs (Fig. 3C). Thus, miR-107 might be a potential biomarker for
250 the development of CAD. Subsequently, we verified miR-107 mimic transfection could
251 up-regulate miR-107 expression in HA-VSMCs relative to miR-NC mimic transfection
252 (Fig. 3D). Then the interaction between hsa_circ_0054633 and miR-107 was analyzed.
253 The dual luciferase reporter assay showed miR-107 mimic reduced the luciferase
254 activity in HA-VSMCs cells transfected with the hsa_circ_0054633-wt (circ-wt) (Fig.
255 3E). RIP assay demonstrated that hsa_circ_0054633 and miR-107 were enriched in
256 Ago2 immunoprecipitates compared with control IgG immunoprecipitates (Fig. 3F).
257 Moreover, HA-VSMCs transfected with the bio-miR-107 showed elevated
258 hsa_circ_0054633 levels but exhibited no changes in bio-NC (Fig. 3G). Besides that,
259 we also observed that hsa_circ_0054633 knockdown up-regulated miR-107 expression
260 in HA-VSMCs (Fig. 3H). Taken together, hsa_circ_0054633 was a sponge of miR-107
261 and negatively regulated its expression.

262 **Hsa_circ_0054633 knockdown alleviates PDGF-BB-induced HA-VSMCs** 263 **dysfunction via targeting miR-107**

264 We further studied whether miR-107 involved in hsa_circ_0054633-mediated HA-

265 VSMC dysfunction. First, HA-VSMCs were transfected with anti-NC or anti-miR-107,
266 and anti-miR-107 transfection significantly reduced the level of miR-107 (Fig. 4A).
267 Next, HA-VSMCs were transfected with si-NC, si-circ#1, si-circ#1 + anti-NC, or si-
268 circ#1 + anti-miR-107 after treatment with PDGF-BB, and qRT-PCR analysis showed
269 hsa_circ_0054633 knockdown elevated miR-107 expression, while this elevation was
270 reduced by miR-107 inhibition (Fig. 4B). After that, functional experiments were
271 conducted and results exhibited that miR-107 inhibition reversed hsa_circ_0054633
272 knockdown-induced reduction of the number of migratory (Fig. 4C) and proliferating
273 cell (Fig. 4D), cell cycle arrest (Fig. 4E), and ROS production (Fig. 4F) in PDGF-BB-
274 treated HA-VSMCs. Western blot analysis displayed that hsa_circ_0054633 down-
275 regulation also decreased PDGF-BB-mediated up-regulation of PCNA, cyclin D1,
276 MMP9, and SOD2, while these down-regulations were rescued by miR-107 inhibition
277 in HA-VSMCs (Fig. 4G). Altogether, hsa_circ_0054633 alleviated PDGF-BB-induced
278 HA-VSMC dysfunction by targeting miR-107.

279 **TXNIP is a target of miR-107**

280 Through searching the starBase program, we found TXNIP contained the binding
281 sites of miR-107 (Fig. 5A). TXNIP expression was found to be up-regulated in the
282 plasma from CAD patients relative to the plasma from healthy people (Fig. 5B), and
283 high expression of TXNIP was linked with symptoms of hypertension, and total
284 cholesterol ≥ 5.1 mmol/L as well as triglyceride ≥ 1.8 mmol/L ($P < 0.05$; Table 2),
285 suggesting TXNIP increase might be associated with the development of CAD.
286 Similarly, TXNIP expression at mRNA and protein levels also increased in PDGF-BB-

287 induced HA-VSMCs (Fig. 5C, D). Afterwards, a decline of luciferase activity in HA-
288 VSMCs cells co-transfected with TXNIP 3'UTR-wt and miR-107 mimic confirmed the
289 direct interaction between TXNIP and miR-107 (Fig. 5E). Subsequent western blot
290 analysis displayed that miR-107 overexpression decreased the level of TXNIP (Fig. 5F,
291 G). These data verified that miR-107 targetedly suppressed TXNIP expression.
292 Importantly, we also observed that hsa_circ_0054633 silencing decreased the level of
293 TXNIP in HA-VSMCs, while this decrease was rescued by miR-107 inhibition (Fig.
294 5H, I), thus hsa_circ_0054633 could indirectly regulate TXNIP expression through
295 miR-107.

296 **Hsa_circ_0054633 moderates PDGF-BB-induced HA-VSMCs damage by** 297 **regulating TXNIP**

298 Given the relationship between hsa_circ_0054633 and TXNIP, we further
299 investigated whether TXNIP participated in the action of hsa_circ_0054633 on HA-
300 VSMCs. First, HA-VSMCs were transfected with TXNIP or vector, by contrast to
301 vector transfection, TXNIP transfection significantly elevated the expression of TXNIP
302 at mRNA and protein levels (Fig. 6A, B). Then HA-VSMCs were transfected with si-
303 NC, si-circ#1, si-circ#1 + vector, or si-circ#1 + TXNIP after treatment with PDGF-BB,
304 we found TXNIP rescued hsa_circ_0054633 knockdown-induced down-regulation of
305 TXNIP expression (Fig. 6C, D), further indicating hsa_circ_0054633 could regulate
306 TXNIP expression. Subsequently, rescued assay showed TXNIP up-regulation reversed
307 hsa_circ_0054633 knockdown-induced migration suppression (Fig. 6E), decreased
308 ROS production (Fig. 6F), and proliferation inhibition (Fig. 6G) and cell cycle arrest

309 (Fig. 6H) in PDGF-BB-treated HA-VSMCs. Besides that, TXNIP up-regulation also
310 elevated the levels of PCNA, cyclin D1, MMP9, and SOD2 mediated by
311 hsa_circ_0054633 knockdown in PDGF-BB-treated HA-VSMCs (Fig. 6I). In all,
312 hsa_circ_0054633 moderated PDGF-BB-induced HA-VSMC dysfunction by
313 regulating TXNIP.

314

315 Discussion

316 VSMC phenotypic switching is an early event in atherosclerosis and neointimal
317 formation, and the involvement of circRNAs in the regulation of phenotypic switching
318 of VSMCs has been identified [18, 19]. For example, circ-Sirt1 suppressed NF- κ B
319 activation by up-regulating SIRT1 expression via sponging miR-132/212 to hinder
320 inflammatory phenotypic switching of VSMCs [20]. Circ-SATB2 promoted VSMC
321 phenotypic proliferation, apoptosis, differentiation and migration through up-regulating
322 STIM1 expression [21]. CircRNA_0020397 enhanced VSMC proliferation via
323 regulating miR-138/KDR axis to alleviate intracranial aneurysm progression [22].
324 Circ_RUSC2 overexpression affected phenotypic modulation of VSMCs by
325 contributing to proliferation, migration and suppressing apoptosis through increasing
326 miR-661-mediated SYK expression [23]. Thus, circRNAs may be important factors in
327 the dysfunction of VSMCs. In this study, hsa_circ_0054633 expression was higher in
328 the plasma of CAD patients than that in healthy individuals, besides, hsa_circ_0054633
329 showed a higher ROC AUC, and might be a potential diagnostic biomarker for early
330 prediction of CAD. Additionally, hsa_circ_0054633 expression was also up-regulated

331 in PDGF-BB-induced cells, suggesting that hsa_circ_0054633 elevation might be
332 associated with the development of CAD. Then functional experiments showed
333 hsa_circ_0054633 silence reversed PDGF-BB-induced promotion on HA-VSMC
334 proliferation, cell cycle, and migration, thereby impeding the formation of
335 atherosclerosis. PCNA is a gene on chromosome 20pter-p12 that encodes a
336 homotrimeric nuclear protein that acts as a processivity factor for DNA polymerase
337 delta in eukaryotic cells and is essential for DNA replication, repair, and recombination
338 [24]. Cyclin D1 (CCND1) is a proto-oncogene located on chromosome 11q13 that is an
339 essential regulator of the G1-S transition in cell cycle control progression [25]. MMP-
340 9 is a matrixin, a class of enzymes that belong to the zinc-metalloproteinases family
341 involved in the degradation of collagens IV and V, gelatins I and V, and fibronectin, and
342 plays a important role in local proteolysis of the extracellular matrix and in leukocyte
343 migration [26]. In this study, western blot analysis indicated hsa_circ_0054633 down-
344 regulation also decreased PDGF-BB-mediated up-regulation of PCNA, cyclin D1 and
345 MMP9 expression, further revealing the involvement of hsa_circ_0054633 in PDGF-
346 BB-induced HA-VSMC dysfunction. ROS always is generated during the
347 inflammatory response, which oxidizes low-density lipoproteins and results in
348 structural damage and dysfunction of endothelial cells, ultimately leads to vascular
349 remodeling [27-29]. Also, the antioxidant system, such as SOD2 enzyme, a
350 mitochondrial enzyme that catalyzes the conversion of $O_2^{\cdot-}$ to hydrogen peroxide
351 (H_2O_2), and the amount of ROS are kept in a certain state of homeostasis [30-32]. In
352 this study, we also found hsa_circ_0054633 silence reversed PDGF-BB-induced ROS

353 production and SOD2 elevation in HA-VSMCs. Thus, hsa_circ_0054633 was
354 important in VSMC homeostasis.

355 MicroRNAs (miRNAs) are a class of small noncoding RNA molecules, which have
356 been revealed to play important roles in multiple cellular processes, including cell
357 proliferation, apoptosis, migration, tumorigenesis, oxidative stress and differentiation
358 [33-35]. Increasing evidence suggests that many miRNAs involve in VSMC phenotypic
359 modulation [36]. MiR-107 is a functional miRNA. Gao *et al.* revealed that miR-107
360 overexpression reduced the level of blood lipid and atherosclerotic index, suppressed
361 vascular endothelial cell (VEC) apoptosis, inflammation and endoplasmic reticulum
362 stress through KRT1-dependent Notch signaling pathway in coronary atherosclerosis
363 [37]. Besides that, miR-107 was found to be decreased in the blood of AS patients, and
364 involved in circRNA-0044073-mediated promotion of the
365 proliferation and invasion of human VSMCs and human VECs [38]. In this study, miR-
366 107 was confirmed to be a target of hsa_circ_0054633. MiR-107 was decreased in HA-
367 VSMCs, and was down-regulated by PDGF-BB and hsa_circ_0054633. What's more,
368 miR-107 inhibition reversed hsa_circ_0054633 silence-mediated inhibition of the
369 proliferation, cell cycle, migration and ROS generation in PDGF-BB-induced HA-
370 VSMCs.

371 TXNIP is an endogenous inhibitor and regulator of thioredoxin (TRX), and
372 modulate oxidative stress via repressing antioxidant activity of TRX [39]. TXNIP is
373 abundant in the vascular wall [40], and involves in controlling vascular neointimal
374 lesion formation [41]. TXNIP promotes Ox-LDL exposure-induced inflammatory

375 injuries of human aortic endothelial cells (HAECs) to contribute to atherosclerotic
376 development [42]. This study found TXNIP was up-regulated in the plasma of CAD
377 patients and PDGF-BB-induced HA-VSMCs. TXNIP was a target of miR-107, and
378 hsa_circ_0054633 served as a competing endogenous RNA for miR-107 to regulate
379 TXNIP expression in HA-VSMCs. Additionally, TXNIP overexpression overturned the
380 inhibitory action of hsa_circ_0054633 knockdown on PDGF-BB-induced HA-VSMC
381 dysfunction.

382 However, although some interesting results have been drawn from our study, there
383 are still some limitations. First, we mainly performed our research work in PDGF-BB-
384 induced HA-VSMC. Further researches should be carried out *in vivo* and a larger cohort
385 of the disease. People may put efforts in making use of animal models with high or low
386 hsa_circ_0054633 expression in mice in the future. Besides that, the involvement of
387 circRNAs in regulating cell functions is very complex, new study should be conducted
388 to explore other potential molecular mechanisms underlying hsa_circ_0054633 in HA-
389 VSMC dysfunction.

390 In conclusion, this study demonstrated that hsa_circ_0054633 knockdown
391 protected HA-VSMCs from PDGF-BB-induced dysfunction through up-regulating
392 miR-107 and subsequent down-regulating TXNIP expression, suggesting a useful
393 strategy for coronary atherosclerosis therapy.

394

395

396

397 **Acknowledgements**

398 Not applicable.

399

400 **Funding**

401 No funding was received.

402

403 **Availability of data and materials**

404 The analyzed data sets generated during the present study are available from the
405 corresponding author on reasonable request.

406

407 **Authors' contribution**

408 Conceptualization, Methodology, Formal analysis and Data curation: Yi Ding and Ye
409 Tian; Validation and Investigation: Xiaochun Lei and Peng Ding; Writing - original
410 draft preparation and Writing - review and editing: Xiaochun Lei, Yi Ding and Peng
411 Ding; Approval of final manuscript: all authors

412

413 **Ethics approval and consent to participate**

414 The present study was approved by the ethical review committee of the Second
415 Affiliated Hospital of Xi'an Medical University.

416

417 **Patient consent for publication**

418 Not applicable.

419

420 **Competing interests**

421 The authors declare that they have no competing interests.

422 **References**

- 423 1. Abubakar I, Tillmann T, Banerjee A. Global, regional, and national age-sex
424 specific all-cause and cause-specific mortality for 240 causes of death, 1990-2013:
425 a systematic analysis for the Global Burden of Disease Study 2013. *Lancet* 2015;
426 385: 117-71.
- 427 2. Koganti S, Eleftheriou D, Brogan P A, Kotecha T, Hong Y, Rakhit R D.
428 Microparticles and their role in coronary artery disease. *Int J Cardiol* 2017; 230:
429 339-45.
- 430 3. Lusis A J. Atherosclerosis. *Nature* 2000; 407: 233-41.
- 431 4. Johnson J L. Emerging regulators of vascular smooth muscle cell function in the
432 development and progression of atherosclerosis. *Cardiovasc Res* 2014; 103: 452-
433 60.
- 434 5. Hutcheson J D, Goettsch C, Bertazzo S, et al. Genesis and growth of extracellular-
435 vesicle-derived microcalcification in atherosclerotic plaques. *Nat Mater* 2016; 15:
436 335.
- 437 6. Qu Y, Zhang N. miR-365b-3p inhibits the cell proliferation and migration of
438 human coronary artery smooth muscle cells by directly targeting ADAMTS1 in
439 coronary atherosclerosis. *Exp Ther Med* 2018; 16: 4239-45.
- 440 7. Barrett S P, Wang P L, Salzman J. Circular RNA biogenesis can proceed through

- 441 an exon-containing lariat precursor. *Elife* 2015; 4: e07540.
- 442 8. Li Z, Huang C, Bao C, et al. Exon-intron circular RNAs regulate transcription in
443 the nucleus. *Nat Struct Mol Biol* 2015; 22: 256.
- 444 9. Ebbesen K K, Kjems J, Hansen T B. Circular RNAs: identification, biogenesis and
445 function. *Biochim Biophys Acta* 2016; 1859: 163-8.
- 446 10. Panda A C, Abdelmohsen K, Gorospe M. SASP regulation by noncoding RNA.
447 *Mech Ageing Dev* 2017; 168: 37-43.
- 448 11. Hombach S, Kretz M. Non-coding RNAs: classification, biology and functioning.
449 *Adv Exp Med Biol* 2016; 937: 3-17.
- 450 12. Ma H, Xu Y, Zhang R, Guo B, Zhang S, Zhang X. Differential expression study
451 of circular RNAs in exosomes from serum and urine in patients with idiopathic
452 membranous nephropathy. *Arch Med Sci* 2019; 15:738-753.
- 453 13. Zhao Z, Li X, Jian D, Hao P, Rao L, Li M. Hsa_circ_0054633 in peripheral blood
454 can be used as a diagnostic biomarker of pre-diabetes and type 2 diabetes mellitus.
455 *Acta Diabetol* 2017; 54: 237-45.
- 456 14. Pan L, Lian W, Zhang X, et al. Human circular RNA0054633 regulates high
457 glucoseinduced vascular endothelial cell dysfunction through the
458 microRNA218/roundabout 1 and microRNA218/heme oxygenase1 axes. *Int J Mol*
459 *Med* 2018; 42: 597-606.
- 460 15. Li X, Zhao Z, Jian D, Li W, Tang H, Li M. Hsa-circRNA11783-2 in peripheral
461 blood is correlated with coronary artery disease and type 2 diabetes mellitus. *Diab*
462 *Vasc Dis Res* 2017; 14: 510-5.

- 463 16. Shawky N M, Segar L. Sulforaphane inhibits platelet-derived growth factor-
464 induced vascular smooth muscle cell proliferation by targeting
465 mTOR/p70S6kinase signaling independent of Nrf2 activation. *Pharmacol Res*
466 2017; 119: 251-64.
- 467 17. Millette E, Rauch B H, Kenagy R D, Daum G, Clowes A W. Platelet-derived
468 growth factor-BB transactivates the fibroblast growth factor receptor to induce
469 proliferation in human smooth muscle cells. *Trends Cardiovasc Med* 2006; 16: 25-
470 8.
- 471 18. Ballantyne M D, Pinel K, Dakin R, et al. Smooth Muscle Enriched Long
472 Noncoding RNA (SMILR) Regulates Cell Proliferation. *Circulation* 2016; 133:
473 2050-65.
- 474 19. Iaconetti C, De Rosa S, Polimeni A, et al. Down-regulation of miR-23b induces
475 phenotypic switching of vascular smooth muscle cells in vitro and in vivo.
476 *Cardiovasc Res* 2015; 107: 522-33.
- 477 20. Kong P, Yu Y, Wang L, et al. circ-Sirt1 controls NF-kappaB activation via
478 sequence-specific interaction and enhancement of SIRT1 expression by binding to
479 miR-132/212 in vascular smooth muscle cells. *Nucleic Acids Res* 2019; 47: 3580-
480 93.
- 481 21. Mao Y Y, Wang J Q, Guo X X, Bi Y, Wang C X. Circ-SATB2 upregulates STIM1
482 expression and regulates vascular smooth muscle cell proliferation and
483 differentiation through miR-939. *Biochem Biophys Res Commun* 2018; 505: 119-
484 25.

- 485 22. Wang Y, Wang Y, Li Y, et al. Decreased expression of circ_0020397 in intracranial
486 aneurysms may be contributing to decreased vascular smooth muscle cell
487 proliferation via increased expression of miR-138 and subsequent decreased KDR
488 expression. *Cell Adh Migr* 2019; 13: 220-8.
- 489 23. Sun J, Zhang Z, Yang S. Circ_RUSC2 upregulates the expression of miR-661
490 target gene SYK and regulates the function of vascular smooth muscle cells.
491 *Biochem Cell Biol* 2019; 97: 709-14.
- 492 24. Park SY, Jeong MS, Han CW, Yu HS, Jang SB. Structural and Functional Insight
493 into Proliferating Cell Nuclear Antigen. *J Microbiol Biotechnol* 2016; 26:637-647.
- 494 25. John RR, Malathi N, Ravindran C, Anandan S. Mini review: Multifaceted role
495 played by cyclin D1 in tumor behavior. *Indian J Dent Res* 2017; 28:187-192.
- 496 26. Makarenkova HP, Meech R. Barx homeobox family in muscle development and
497 regeneration. *Int Rev Cell Mol Biol* 2012; 297:117-173.
- 498 27. Zhang Y, Huang J, Yang X, et al. Altered Expression of TXNIP in the peripheral
499 leukocytes of patients with coronary atherosclerotic heart disease. *Medicine* 2017;
500 96: e9108.
- 501 28. Derosa G, Maffioli P, D'Angelo A, Russo R. Effects of a nutraceutical combination
502 of monacolin, γ -oryzanol and γ -aminobutyric acid on lipid profile and C-reactive
503 protein in mice. *Arch Med Sci* 2019, 15:792.
- 504 29. Pavlović I, Pejić S, Radojević-Škodrić S, et al. The effect of antioxidant status on
505 overall survival in renal cell carcinoma. *Arch Med Sci* 2020, 16:94.
- 506 30. Chang D, Zhang X, Rong S, et al. Serum antioxidative enzymes levels and

- 507 oxidative stress products in age-related cataract patients. *Oxid Med Cell Longev*
508 2013; 2013:587826.
- 509 31. Kaczmarczyk-Sedlak I, Folwarczna J, Sedlak L, et al. Effect of caffeine on
510 biomarkers of oxidative stress in lenses of rats with streptozotocin-induced
511 diabetes. *Arch Med Sci* 2019, 15:1073.
- 512 32. Klisic A, Kavacic N, Stanistic V, et al. Endocan and a novel score for dyslipidemia,
513 oxidative stress and inflammation (DOI score) are independently correlated with
514 glycated hemoglobin (HbA1c) in patients with prediabetes and type 2 diabetes.
515 *Arch Med Sci* 2020, 16:42.
- 516 33. Cheng A M, Byrom M W, Shelton J, Ford L P. Antisense inhibition of human
517 miRNAs and indications for an involvement of miRNA in cell growth and
518 apoptosis. *Nucleic Acids Res* 2005; 33: 1290-7.
- 519 34. Chen C-Z, Li L, Lodish H F, Bartel D P. MicroRNAs modulate hematopoietic
520 lineage differentiation. *Science* 2004; 303: 83-6.
- 521 35. Banerjee J, Khanna S, Bhattacharya A. MicroRNA Regulation of Oxidative Stress.
522 *Oxid Med Cell Longev* 2017; 2017: 2872156.
- 523 36. Guo X, Li D, Chen M, et al. miRNA-145 inhibits VSMC proliferation by targeting
524 CD40. *Sci Rep* 2016; 6: 35302.
- 525 37. Gao Z F, Ji X L, Gu J, Wang X Y, Ding L, Zhang H. microRNA - 107 protects
526 against inflammation and endoplasmic reticulum stress of vascular endothelial
527 cells via KRT1 - dependent Notch signaling pathway in a mouse model of
528 coronary atherosclerosis. *J Cell Physiol* 2019; 234: 12029-41.

- 529 38. Shen L, Hu Y, Lou J, et al. CircRNA-0044073 is upregulated in atherosclerosis
530 and increases the proliferation and invasion of cells by targeting miR-107. Mol
531 Med Rep 2019; 19: 3923-32.
- 532 39. Devi T S, Hosoya K-I, Terasaki T, Singh L P. Critical role of TXNIP in oxidative
533 stress, DNA damage and retinal pericyte apoptosis under high glucose:
534 implications for diabetic retinopathy. Exp Cell Res 2013; 319: 1001-12.
- 535 40. Berk B C. Novel approaches to treat oxidative stress and cardiovascular diseases.
536 Trans Am Clin Climatol Assoc 2007; 118: 209.
- 537 41. Perrone L, Devi T S, Hosoya K i, Terasaki T, Singh L P. Thioredoxin interacting
538 protein (TXNIP) induces inflammation through chromatin modification in retinal
539 capillary endothelial cells under diabetic conditions. J Cell Physiol 2009; 221:
540 262-72.
- 541 42. Chen M, Li W, Zhang Y, Yang J. MicroRNA-20a protects human aortic endothelial
542 cells from Ox-LDL-induced inflammation through targeting TLR4 and TXNIP
543 signaling. Biomed Pharmacother 2018; 103: 191-7.

544

545

546 **Figure legends**

547 **Fig. 1 Hsa_circ_0054633 expression is elevated in CAD patients and PDGF-BB-**
548 **induced HA-VSMCs.** (A) The expression of hsa_circ_0054633 was detected in the
549 plasma from CAD patients and healthy people using qRT-PCR. (B) ROC curves were
550 plotted to determine the diagnostic value of hsa_circ_0054633 in plasma of CAD

551 patients. (C) The expression of hsa_circ_0054633 was measured in HA-VSMCs treated
552 with or without PDGF-BB by qRT-PCR. * P <0.05, ** P <0.01.

553 **Fig. 2 Hsa_circ_0054633 knockdown reverses PDGF-BB-induced HA-VSMCs**
554 **dysfunction.** (A) qRT-PCR analysis of hsa_circ_0054633 expression in HA-VSMCs
555 transfected with two forms of si-hsa_circ_0054633. HA-VSMCs were treated with
556 PDGF-BB, PDGF-BB + si-NC, or PDGF-BB + si-circ#1. After treatment, (B) qRT-
557 PCR analysis of hsa_circ_0054633 expression in HA-VSMCs; (C) CCK-8 assay of
558 HA-VSMC proliferation; (D) flow cytometric analysis of cell cycle in HA-VSMCs; (E)
559 transwell analysis of HA-VSMC migration; (F) ROS generation analysis of HA-
560 VSMCs with DCFH-DA assay; (G) western blot analysis of PCNA, cyclin D1, MMP9,
561 and SOD2 expression in HA-VSMCs. * P <0.05, ** P <0.01.

562 **Fig. 3 Hsa_circ_0054633 is a sponge of miR-107.** (A) The putative binding sequences
563 of miR-107 on hsa_circ_0054633. (B) qRT-PCR analysis of miR-107 expression in the
564 plasma from CAD patients and healthy people. (C) qRT-PCR analysis of miR-107
565 expression in HA-VSMCs treated with or without PDGF-BB. (D) qRT-PCR analysis of
566 miR-107 in HA-VSMCs transfected with miR-NC or miR-107. (E) Dual-luciferase
567 reporter assay in HA-VSMCs co-transfected with hsa_circ_0054633-wt or
568 hsa_circ_0054633-mut and the indicated miRNAs. (F) RIP assay for the enrichment of
569 Ago2 on circ_0054633 and miR-107 in HA-VSMCs. (G) qRT-PCR analysis of
570 hsa_circ_0054633 level in the materials pulled down by bio-miR-107. (H) qRT-PCR
571 analysis of miR-107 level in HA-VSMCs transfected with si-NC or si-circ#1. * P <0.05,
572 ** P <0.01.

573 **Fig. 4 Hsa_circ_0054633 knockdown alleviates PDGF-BB-induced HA-VSMCs**
574 **dysfunction via targeting miR-107.** (A) qRT-PCR analysis of miR-107 level in HA-
575 VSMCs transfected with anti-NC or anti-miR-107. HA-VSMCs were transfected with
576 si-NC, si-circ#1, si-circ#1 + anti-NC, or si-circ#1 + anti-miR-107 after treatment with
577 PDGF-BB. After transfection, (B) qRT-PCR analysis of miR-107 level in HA-VSMCs;
578 (C) HA-VSMC migration analysis with transwell assay; (D) proliferation analysis of
579 HA-VSMCs with CCK-8 assay; (E) cell cycle detection of HA-VSMCs with flow
580 cytometry; (F) DCFH-DA assay of ROS generation in HA-VSMCs; (G) the detection
581 of PCNA, cyclin D1, MMP9, and SOD2 expression in HA-VSMCs using western blot.
582 * $P < 0.05$.

583 **Fig. 5 TXNIP is a target of miR-107.** (A) The putative binding sequences of miR-107
584 on TXNIP 3'UTR. (B) qRT-PCR analysis of TXNIP expression in the plasma from
585 CAD patients and healthy people. (C, D) TXNIP expression measurement in HA-
586 VSMCs treated with or without PDGF-BB using qRT-PCR and western blot. (E) Dual-
587 luciferase reporter assay in HA-VSMCs co-transfected with TXNIP 3'UTR-wt or -mut
588 and miR-107 or miR-NC. (F, G) TXNIP expression detection in HA-VSMCs
589 transfected with miR-NC or miR-107 using qRT-PCR and western blot. (H, I) TXNIP
590 expression detection in HA-VSMCs transfected with si-NC, si-circ#1, si-circ#1 + anti-
591 NC, or si-circ#1 + anti-miR-107 using qRT-PCR and western blot. * $P < 0.05$, ** $P < 0.01$.

592 **Fig. 6 Hsa_circ_0054633 moderates PDGF-BB-induced HA-VSMCs damage by**
593 **regulating TXNIP.** (A, B) TXNIP expression detection in HA-VSMCs transfected with
594 vector or TXNIP with qRT-PCR and western blot. HA-VSMCs were transfected with

595 si-NC, si-circ#1, si-circ#1 + vector, or si-circ#1 + TXNIP after treatment with PDGF-
596 BB. After transfection, (C, D) TXNIP expression detection in HA-VSMCs using qRT-
597 PCR and western blot. (E) transwell assay of HA-VSMC migration; (F) ROS generation
598 analysis of HA-VSMCs with DCFH-DA assay; (G) CCK-8 assay of proliferation in
599 HA-VSMCs; (H) flow cytometric analysis of cell cycle in HA-VSMCs; (I) western blot
600 analysis of PCNA, cyclin D1, MMP9, and SOD2 levels in HA-VSMCs. * $P < 0.05$,
601 ** $P < 0.01$.

602

603 **Table 1. The clinical and demographic characteristics of the patients with CAD**
604 **and Controls.**

605 **Table 2. Correlation of the expression of hsa_circ_0054633/ miR-107/TXNIP with**
606 **clinicopathologic features in patients of CAD**

607

608

609

Table 1. The clinical and demographic characteristics of the patients with CAD and Controls.

| | Normal(n=33) | CAD(n=33) | <i>P</i> value |
|--------------------------------------|--------------|------------|----------------|
| Males/females | 15/18 | 19/14 | 0.33 |
| Age (years) | 56.1 ± 5.6 | 57.5 ± 6.1 | 0.34 |
| Body mass index (kg/m ²) | 22.4 ± 2.2 | 23.8 ± 2.5 | 0.02 |
| Smokers %(n) | 32.3(11) | 48.5(16) | 0.21 |
| Drinking %(n) | 24.2(8) | 21.2(7) | 0.77 |
| Hypertension %(n) | 12.1(4) | 60.6(20) | <0.01 |
| Diabetes mellitus %(n) | 6.1(2) | 27.2(9) | 0.02 |
| Total cholesterol (mmol/L) | 4.3 ± 1.1 | 5.1 ± 1.3 | <0.01 |
| Triglyceride (mmol/L) | 1.3 ± 0.4 | 1.8 ± 0.6 | <0.01 |
| HDL-C(mmol/L) | 1.2 ± 0.3 | 1.1 ± 0.4 | 0.26 |
| LDL-C(mmol/L) | 2.9 ± 0.8 | 2.1 ± 0.6 | <0.01 |
| Hs-CRP (mg/L) | 1.6 ± 0.7 | 3.2 ± 1.7 | <0.01 |

HDL-C, high-density lipoprotein cholesterol; LDL-C, low density lipoprotein Cholesterol; Hs-CRP: high-sensitivity C-reactive protein.

Data are represented as mean ± SD or number (percentage) for category variables.

P: CAD vs. Normal

Table 2. Correlation of the expression of hsa_circ_0054633/ miR-107/TXNIP with clinicopathologic features in patients of CAD

| Parameters | hsa_circ_0054633 | | | | miR-107 | | | TXNIP | | |
|--------------------------|------------------|------|------|-----------------|------------|------|------|------------|------|-----------------|
| | expression | | | | expression | | | expression | | |
| | High | Low | | <i>p</i> -value | High | Low | | High | Low | <i>p</i> -value |
| | N=33 | N=17 | N=16 | | N=17 | N=16 | | N=17 | N=16 | |
| Gender | | | | | | | | | | |
| Male | 19 | 9 | 10 | 0.58 | 10 | 9 | 0.88 | 8 | 11 | 0.21 |
| Female | 14 | 8 | 6 | | 7 | 7 | | 9 | 5 | |
| Age,years | | | | | | | | | | |
| <60 | 14 | 5 | 9 | 0.12 | 7 | 7 | 0.88 | 8 | 6 | 0.31 |
| ≥60 | 19 | 12 | 7 | | 10 | 9 | | 9 | 10 | |
| Smoking | | | | | | | | | | |
| Positive | 16 | 12 | 4 | <0.01 | 5 | 11 | 0.02 | 10 | 6 | 0.22 |
| Negative | 17 | 5 | 12 | | 12 | 5 | | 7 | 10 | |
| Drinking | | | | | | | | | | |
| Positive | 7 | 6 | 1 | 0.11 | 2 | 5 | 0.35 | 5 | 2 | 0.45 |
| Negative | 26 | 11 | 15 | | 15 | 11 | | 12 | 14 | |
| Hypertension | | | | | | | | | | |
| Positive | 20 | 14 | 6 | <0.01 | 7 | 13 | 0.02 | 15 | 5 | <0.01 |
| Negative | 13 | 3 | 10 | | 10 | 3 | | 2 | 11 | |
| Diabetes mellitus | | | | | | | | | | |
| Positive | 9 | 8 | 1 | 0.03 | 2 | 7 | 0.10 | 7 | 2 | 0.15 |
| Negative | 24 | 9 | 15 | | 15 | 9 | | 10 | 14 | |

| | | | | | | | | | | |
|-------------------|----|----|----|-------|----|----|-------|----|----|-------|
| Total cholesterol | | | | | | | | | | |
| (mmol/L) | | | | | | | | | | |
| ≥5.1 | 16 | 13 | 3 | <0.01 | 5 | 11 | 0.02 | 14 | 2 | <0.01 |
| <5.1 | 17 | 4 | 13 | | 12 | 5 | | 3 | 14 | |
| Triglyceride | | | | | | | | | | |
| (mmol/L) | | | | | | | | | | |
| ≥1.8 | 15 | 12 | 3 | <0.01 | 4 | 11 | <0.01 | 13 | 2 | <0.01 |
| <1.8 | 18 | 5 | 13 | | 13 | 5 | | 4 | 14 | |

Preprint

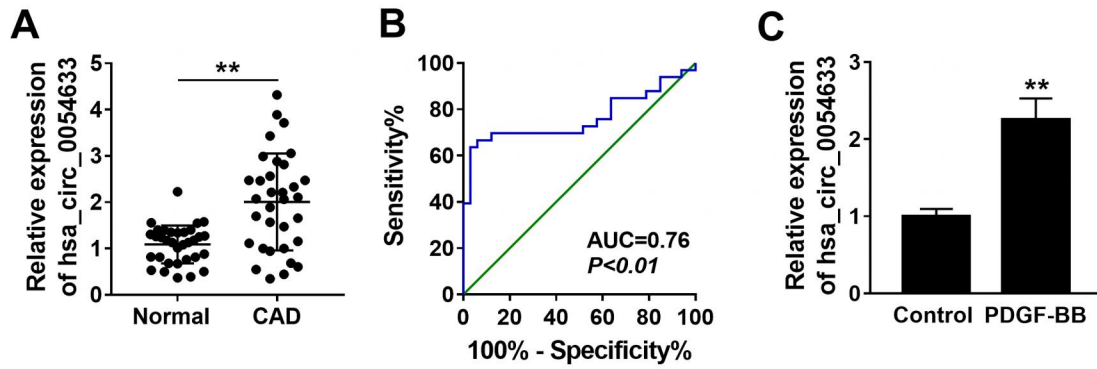


Fig. 1 Hsa_circ_0054633 expression is elevated in CAD patients and PDGF-BB-induced HA-VSMCs. (A) The expression of hsa_circ_0054633 was detected in the plasma from CAD patients and healthy people using qRT-PCR. (B) ROC curves were plotted to determine the diagnostic value of hsa_circ_0054633 in plasma of CAD patients. (C) The expression of hsa_circ_0054633 was measured in HA-VSMCs treated with or without PDGF-BB by qRT-PCR. *P<0.05, **P<0.01.

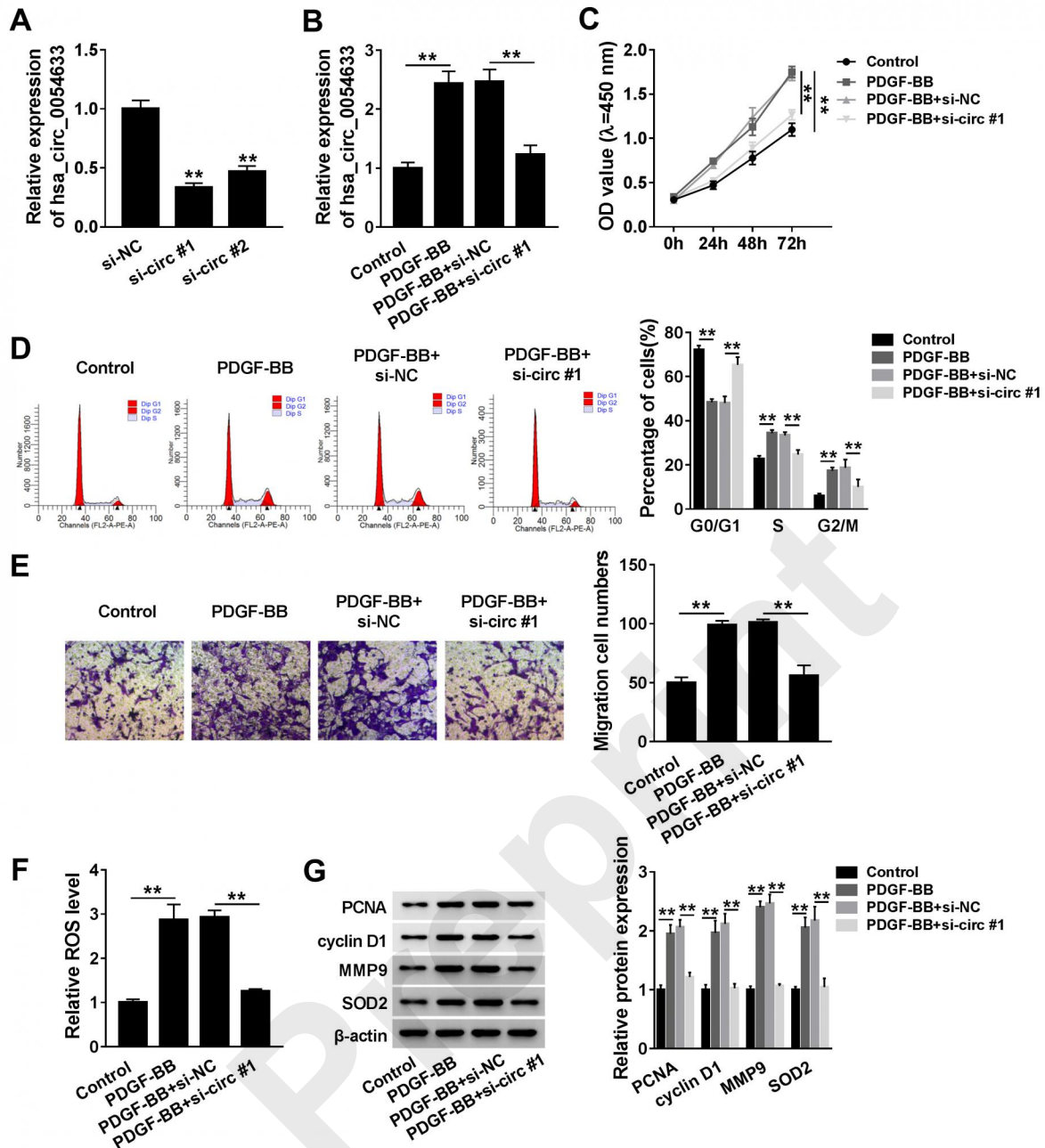


Fig. 2 Hsa_circ_0054633 knockdown reverses PDGF-BB-induced HA-VSMCs dysfunction. (A) qRT-PCR analysis of hsa_circ_0054633 expression in HA-VSMCs transfected with two forms of si-hsa_circ_0054633. HA-VSMCs were treated with PDGF-BB, PDGF-BB + si-NC, or PDGF-BB + si-circ#1. After treatment, (B) qRT-PCR analysis of hsa_circ_0054633 expression in HA-VSMCs; (C) CCK-8 assay of HA-VSMC proliferation; (D) flow cytometric analysis of cell cycle in HA-VSMCs; (E) transwell analysis of HA-VSMC migration; (F) ROS generation analysis of HA-VSMCs with DCFH-DA assay; (G) western blot analysis of PCNA, cyclin D1, MMP9, and SOD2 expression in HA-VSMCs. *P<0.05, **P<0.01.

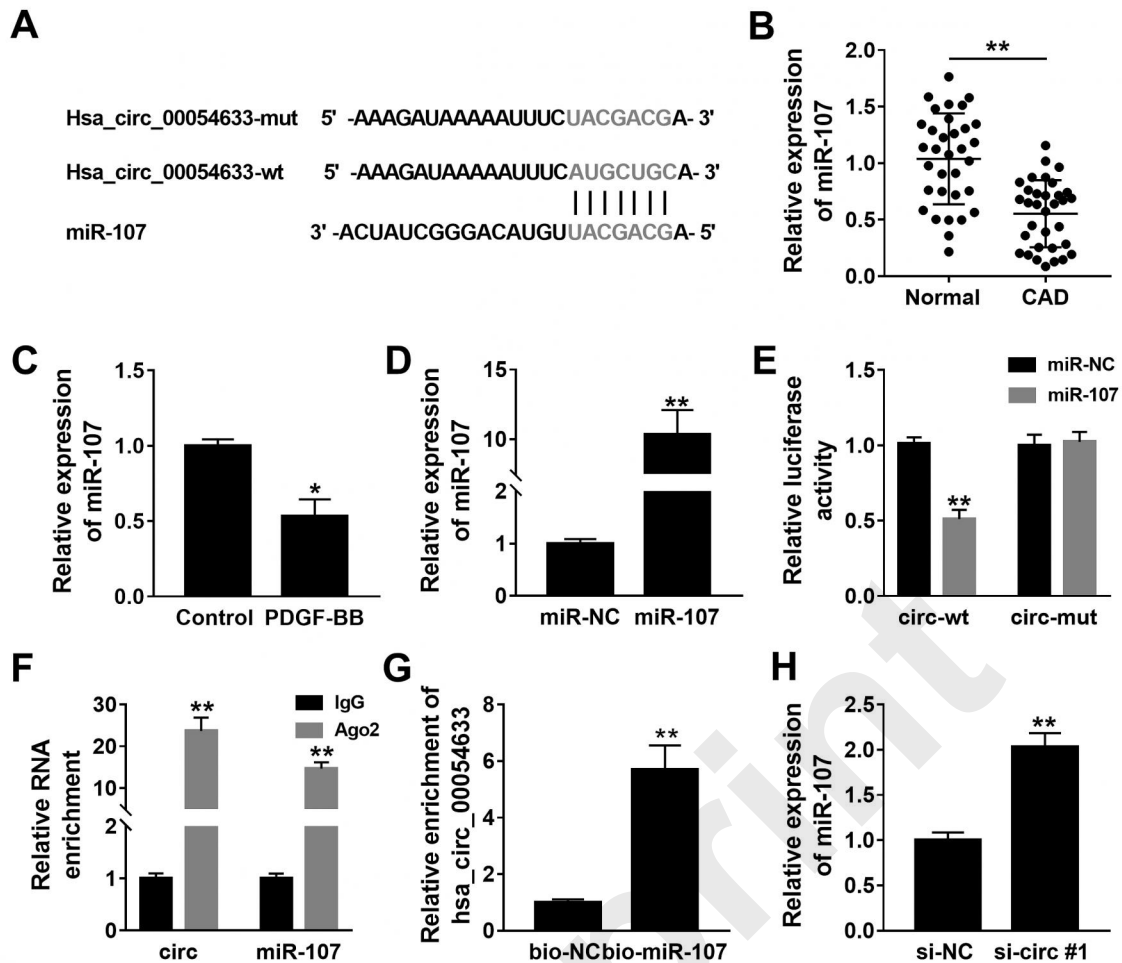


Fig. 3 Hsa_circ_0054633 is a sponge of miR-107. (A) The putative binding sequences of miR-107 on hsa_circ_0054633. (B) qRT-PCR analysis of miR-107 expression in the plasma from CAD patients and healthy people. (C) qRT-PCR analysis of miR-107 expression in HA-VSMCs treated with or without PDGF-BB. (D) qRT-PCR analysis of miR-107 in HA-VSMCs transfected with miR-NC or miR-107. (E) Dual-luciferase reporter assay in HA-VSMCs co-transfected with hsa_circ_0054633-wt or hsa_circ_0054633-mut and the indicated miRNAs. (F) RIP assay for the enrichment of Ago2 on circ_0054633 and miR-107 in HA-VSMCs. (G) qRT-PCR analysis of hsa_circ_0054633 level in the materials pulled down by bio-miR-107. (H) qRT-PCR analysis of miR-107 level in HA-VSMCs transfected with si-NC or si-circ#1. * $P < 0.05$, ** $P < 0.01$.

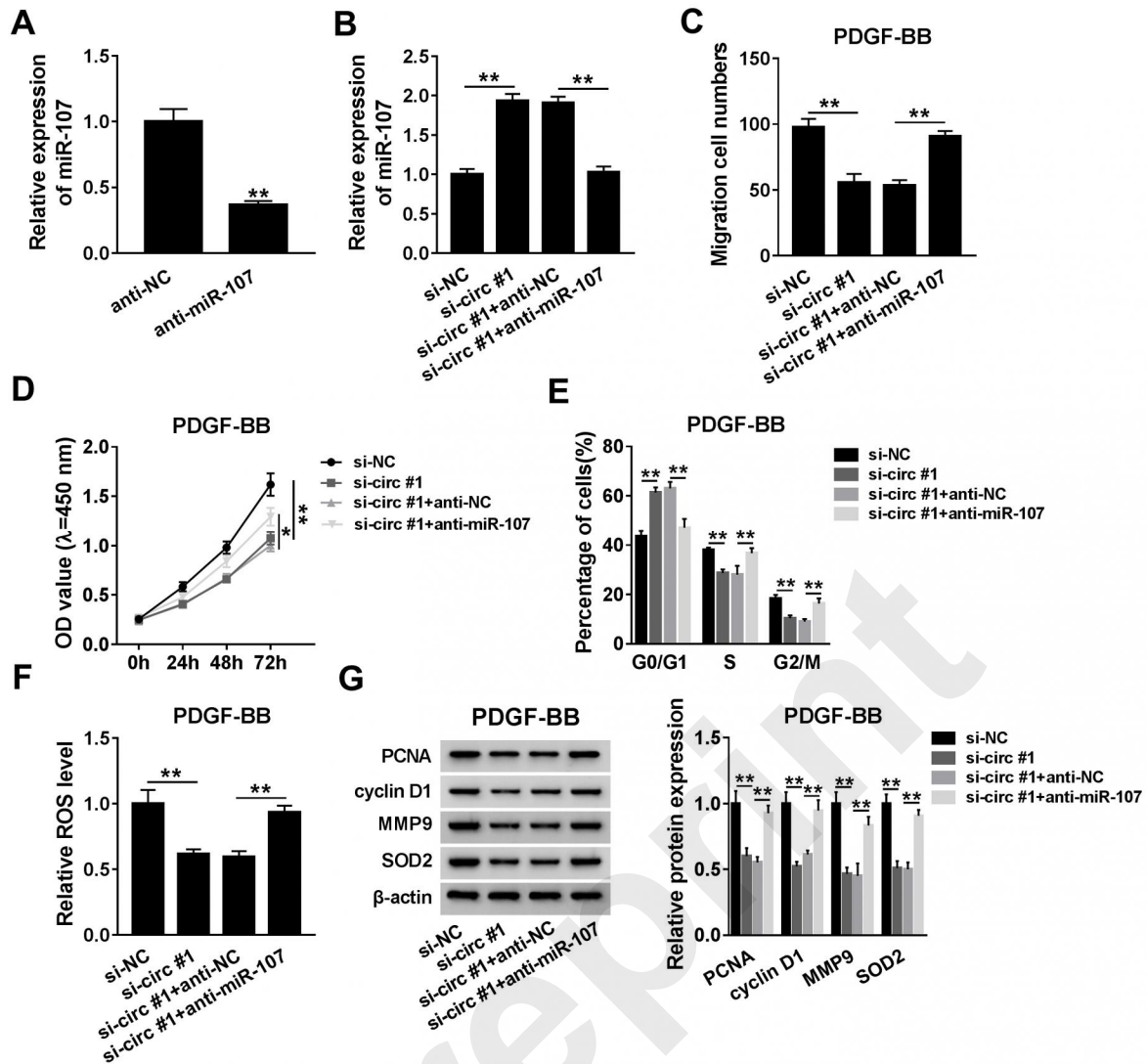


Fig. 4 Hsa_circ_0054633 knockdown alleviates PDGF-BB-induced HA-VSMCs dysfunction via targeting miR-107. (A) qRT-PCR analysis of miR-107 level in HA-VSMCs transfected with anti-NC or anti-miR-107. HA-VSMCs were transfected with si-NC, si-circ#1, si-circ#1 + anti-NC, or si-circ#1 + anti-miR-107 after treatment with PDGF-BB. After transfection, (B) qRT-PCR analysis of miR-107 level in HA-VSMCs; (C) HA-VSMC migration analysis with transwell assay; (D) proliferation analysis of HA-VSMCs with CCK-8 assay; (E) cell cycle detection of HA-VSMCs with flow cytometry; (F) DCFH-DA assay of ROS generation in HA-VSMCs; (G) the detection of PCNA, cyclin D1, MMP9, and SOD2 expression in HA-VSMCs using western blot. *P<0.05.

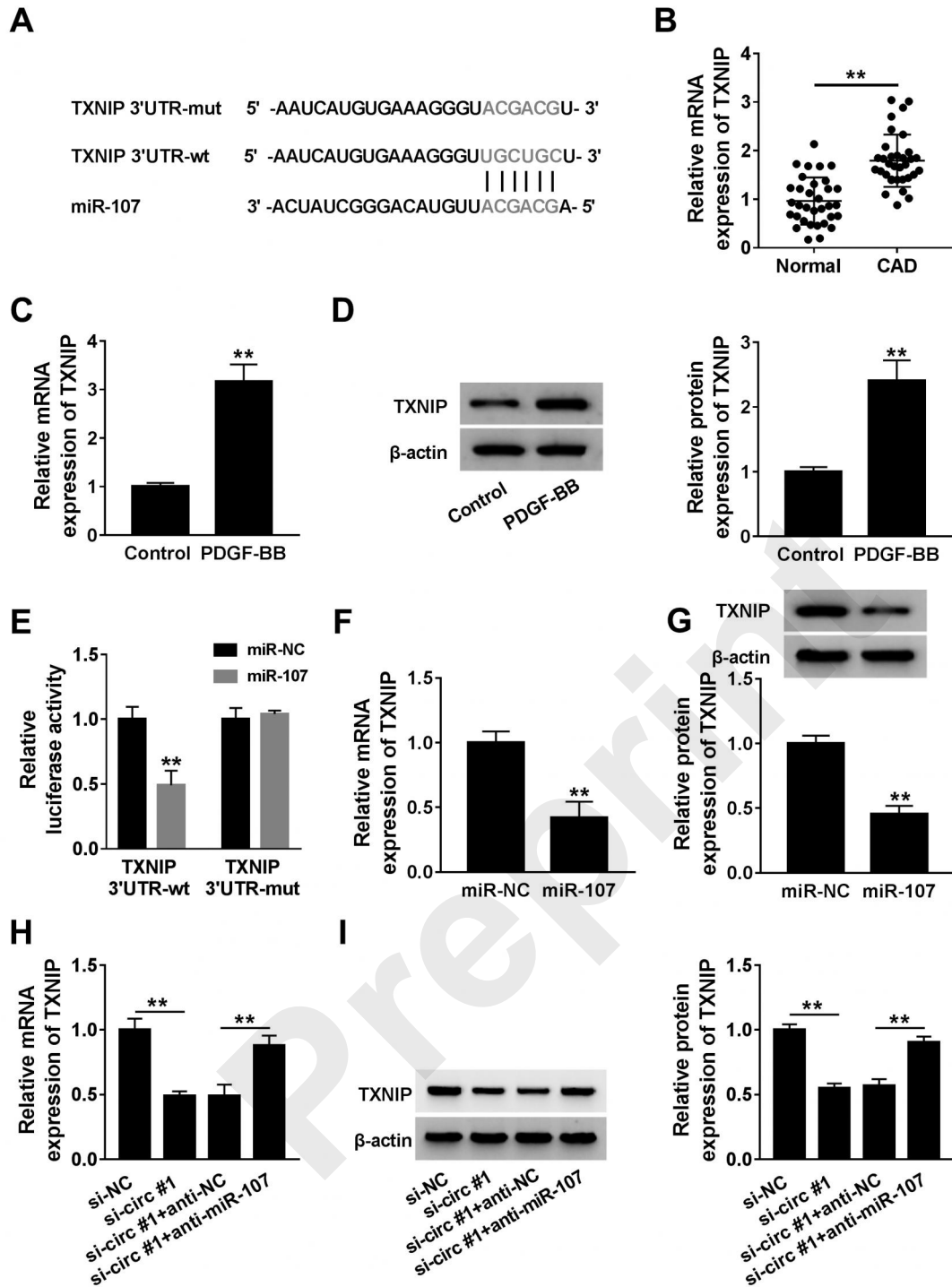


Fig. 5 TXNIP is a target of miR-107. (A) The putative binding sequences of miR-107 on TXNIP 3'UTR. (B) qRT-PCR analysis of TXNIP expression in the plasma from CAD patients and healthy people. (C, D) TXNIP expression measurement in HA-VSMCs treated with or without PDGF-BB using qRT-PCR and western blot. (E) Dual-luciferase reporter assay in HA-VSMCs co-transfected with TXNIP 3'UTR-wt or -mut and miR-107 or miR-NC. (F, G) TXNIP expression detection in HA-VSMCs transfected with miR-NC or miR-107 using qRT-PCR and western blot. (H, I) TXNIP expression detection in HA-VSMCs transfected with si-NC, si-circ#1, si-circ#1 + anti-NC, or si-circ#1 + anti-miR-107 using qRT-PCR and western blot. * $P < 0.05$, ** $P < 0.01$.

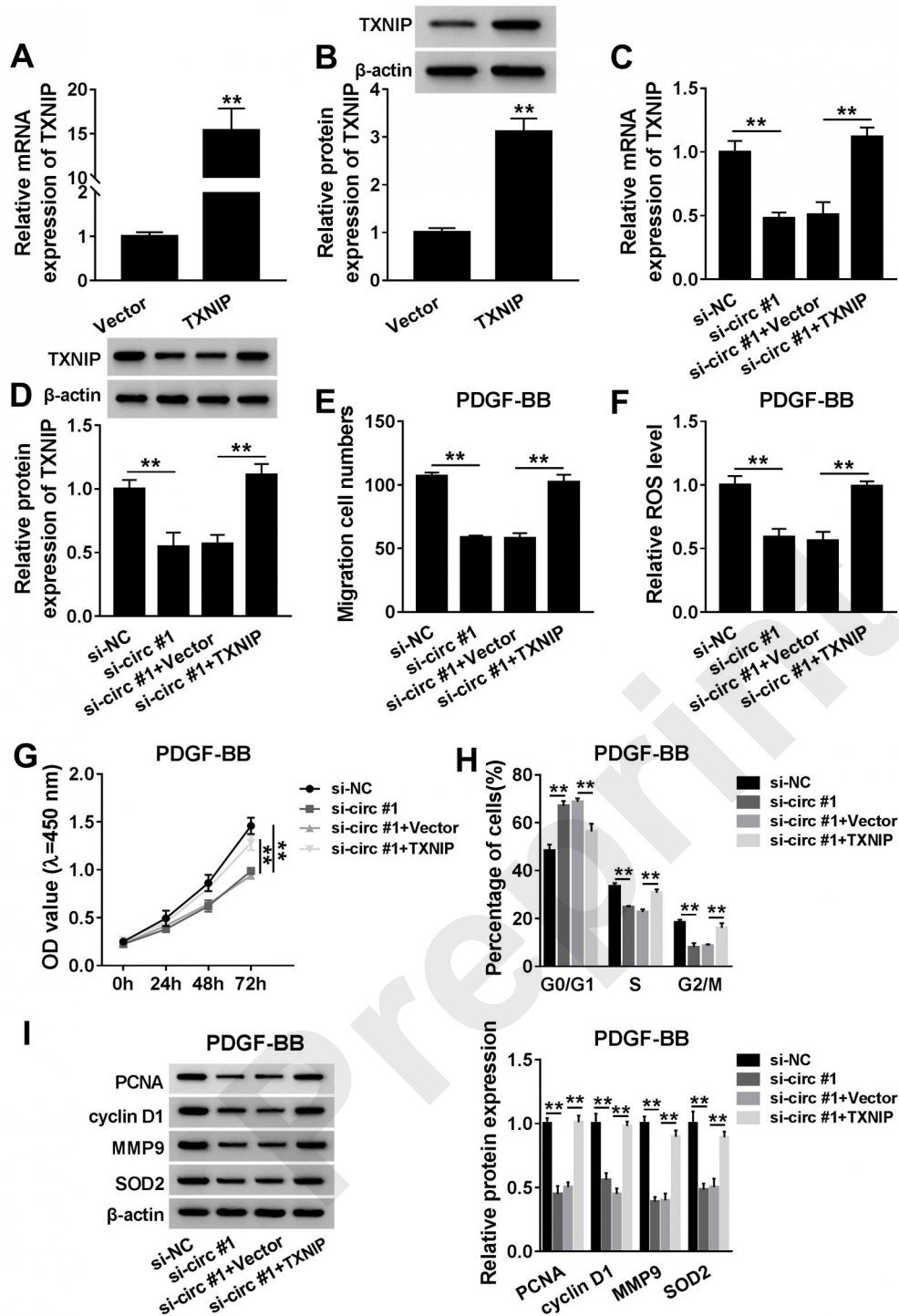


Fig. 6 Hsa_circ_0054633 moderates PDGF-BB-induced HA-VSMCs damage by regulating TXNIP. (A, B) TXNIP expression detection in HA-VSMCs transfected with vector or TXNIP with qRT-PCR and western blot. HA-VSMCs were transfected with si-NC, si-circ#1, si-circ#1 + vector, or si-circ#1 + TXNIP after treatment with PDGF-BB. After transfection, (C, D) TXNIP expression detection in HA-VSMCs using qRT-PCR and western blot. (E) transwell assay of HA-VSMC migration; (F) ROS generation analysis of HA-VSMCs with DCFH-DA assay; (G) CCK-8 assay of proliferation in HA-VSMCs; (H) flow cytometric analysis of cell cycle in HA-VSMCs; (I) western blot analysis of PCNA, cyclin D1, MMP9, and SOD2 levels in HA-VSMCs. * $P < 0.05$, ** $P < 0.01$.